RSC Advances

PAPER

View Article Online
View Journal | View Issue

Cite this: *RSC Adv.*, 2016, **6**, 64871

Highly improved dielectric properties of polymer/α-Fe_2O_3 composites at elevated temperatures

Kenichi Hayashida

α-Fe_2O_3 particles were incorporated into ten kinds of polymer matrices, and the dielectric properties of the resultant polymer/α-Fe_2O_3 composites were investigated between 40 °C and 160 °C. We found that the dielectric properties strongly depended not only on the temperatures but also on the kind of polymer matrices. For engineering plastics such as polyetherimide (PEI), the dielectric constant ε'_r was highly enhanced at around 1 kHz by incorporation of the α-Fe_2O_3 particles owing to Maxwell–Wagner polarization of free electrons in the α-Fe_2O_3 particles. This is probably because the π electrons in the aromatic structures of the engineering plastics strongly interact with the electrons in the α-Fe_2O_3 particles. Furthermore, the dielectric loss factor ε''_r for the engineering plastics became small at elevated temperatures because the conductivity of the α-Fe_2O_3 particle was enhanced and therefore the relaxation frequency of Maxwell–Wagner polarization was shifted to higher frequency. PEI/α-Fe_2O_3 composites exhibited highly improved dielectric properties at around 1 kHz, the high ε'_r and very low ε''_r at the elevated temperatures above 120 °C. It was demonstrated that the PEI/α-Fe_2O_3 composite was comparable to the PEI/$BaTiO_3$ composite in dielectric performance at 160 °C. Because the cost of α-Fe_2O_3 is much lower than that of $BaTiO_3$, the PEI/α-Fe_2O_3 composite might be promising as a low-cost dielectric material for high-temperature applications.

Received 16th May 2016
Accepted 3rd July 2016

DOI: 10.1039/c6ra12752e

www.rsc.org/advances

Introduction

Dielectric materials are mainly used in capacitors to store electrical energy.[1–3] In comparison to ceramic materials, polymer ones have the advantages of low cost, lightweight and high processability. However, the very low dielectric constant ε'_r of the polymer material strongly prevents improvement of the capacitors. Therefore, polymer/ceramic composite materials have been much studied over the last few decades. Among the ceramics, $BaTiO_3$ has been most widely used for enhancement in the ε'_r of polymer materials because of the very high ε'_r of $BaTiO_3$.[4–21] However, the high cost of $BaTiO_3$ is a serious problem for industrial applications.

On the other hand, hematite (α-Fe_2O_3) is a very low cost ceramic material although α-Fe_2O_3 has not been paid attention as a high ε'_r filler for polymer materials owing to the low ε'_r of α-Fe_2O_3; according to the reported literature, the ε'_r of α-Fe_2O_3 is as low as 30.[22–27] Therefore, few studies are available on the dielectric properties of polymer/α-Fe_2O_3 composites.[28–30] Djoković and coworkers reported dielectric properties of a composites epoxy resin and α-Fe_2O_3 nanorods.[28] Also, α-Fe_2O_3 nanorods were dispersed in a poly(vinyl alcohol)/poly(ethylene glycol) blend by Sayed *et al.*[29] There are only small improvements of the ε'_rs of the polymer materials in these studies.

In this paper, we focus on the conductivity σ of α-Fe_2O_3 at elevated temperatures. Typically, α-Fe_2O_3 is known to have σ of about 10^{-5} to 10^{-6} S cm^{-1} at room temperature.[26] The σ of semiconductors such as α-Fe_2O_3 is enhanced as temperature is raised because electrons are excited from a valence band to a conductive band.[31] It is expected that the σ of α-Fe_2O_3 is especially increased owing to its narrow band gap of 2.1 eV.[32] At elevated temperatures, the enhanced σ of the α-Fe_2O_3 particles would bring a high ε'_r to a polymer/α-Fe_2O_3 composite owing to Maxwell–Wagner polarization[33] of the resultant free electrons in the α-Fe_2O_3 particles. The polymer/α-Fe_2O_3 composite might be promising as a low-cost dielectric material for high-temperature applications such as hybrid and electric vehicles.[34,35] In this study, α-Fe_2O_3 particles were incorporated into ten kinds of polymer matrices, and the dielectric properties of the polymer/α-Fe_2O_3 composites were investigated between 40 °C and 160 °C. We found that the dielectric properties strongly depended not only on the temperatures but also on the kind of polymer matrices. Furthermore, the dielectric performance of one of the polymer/α-Fe_2O_3 composite was compared with that of a corresponding polymer/$BaTiO_3$ composite at the elevated temperatures.

Experimental

Sample preparation

α-Fe_2O_3 particles were obtained from Kanto Chemical (Japan). The density and specific area of the α-Fe_2O_3 particles were

Materials and Processing Dept. II, Toyota Central R&D Labs., Inc., Nagakute, Aichi 480-1192, Japan. E-mail: e1440@mosk.tytlabs.co.jp

determined to be 4.94 g cm^{-3} and 8.71 m^2 g^{-1} using helium pycnometry and a standard BET method, respectively. The average diameter of the α-Fe_2O_3 particles was calculated to be 139 nm from the obtained density and specific area data. In the same manner, the density, specific area and average diameter of $BaTiO_3$ particles obtained from Wako Pure Chemical Industries (Japan) were determined to be 5.73 g cm^{-3}, 9.99 m^2 g^{-1} and 105 nm, respectively.

Polystyrene (PS) and poly(methyl methacrylate) (PMMA) were purchased from Wako Pure Chemical Industries (Japan). Poly(2-vinylpyridine) (P2VP) was obtained from Scientific Polymer Products. Styrene/acrylonitrile copolymer (SAN) with 30 wt% of acrylonitrile, polyphenylene ether (PPE), polysulfone (PSF), polyethersulfone (PES) and polyetherimide (PEI) were purchased from Sigma-Aldrich. Styrene/*N*-phenylmaleimide alternating copolymer (St-PMI)[36] and polyarylate (PAR)[37] were synthesized using reported methods, where PAR contained equimolar amounts of isophthaloyl and terephthaloyl moieties.

A series of polymer/α-Fe_2O_3 composites were prepared by simply blending the α-Fe_2O_3 particles with the polymer matrices. First, the α-Fe_2O_3 particles and the polymer matrix except PES were homogeneously dispersed in 1,4-dioxane by sonication. The dispersion was quickly frozen by liquid nitrogen, and then freeze-dried under vacuum. For preparation of PES/α-Fe_2O_3 composites, dichloromethane was used instead of 1,4-dioxane because PES was insoluble in 1,4-dioxane. Subsequently, all the pre-mixtures thus-obtained were further kneaded in molten states. Also, PEI/$BaTiO_3$ composites were prepared in the same manner. The resultant composites were hot-pressed into disklike specimens with a diameter of 33 mm and a thickness of ~0.52 mm. For electrical measurements, two gold electrodes with a diameter of 27 mm were deposited on the top and bottom of the specimens.

Measurements

Complex permittivity was obtained in the frequency *f* range of 10^2 to 10^6 Hz at 2 V using an LCR meter (E4980A, Agilent) coupled with a rheometer (ARES G2, TA instruments). The temperature of the specimen was controlled in the oven of the rheometer. Direct current (DC) resistance of the specimen was measured at room temperature under a nitrogen atmosphere using a megohmmeter (SM-8220, Hioki), and the value was recorded after 10 minute from application of a voltage of 500 V. The cross-section of the specimen that had been flattened with argon ion beam[38] was observed using an SEM (S-4300, Hitachi) operated at an accelerating voltage of 2 kV.

Results and discussion

Dielectric properties of polymer/α-Fe_2O_3 composites at 40 °C

We prepared a series of polymer/α-Fe_2O_3 composites with the volume fraction Φ of α-Fe_2O_3, $\Phi = 0.2$. The chemical structures of the polymer matrices are shown in Fig. 1. All the polymers are

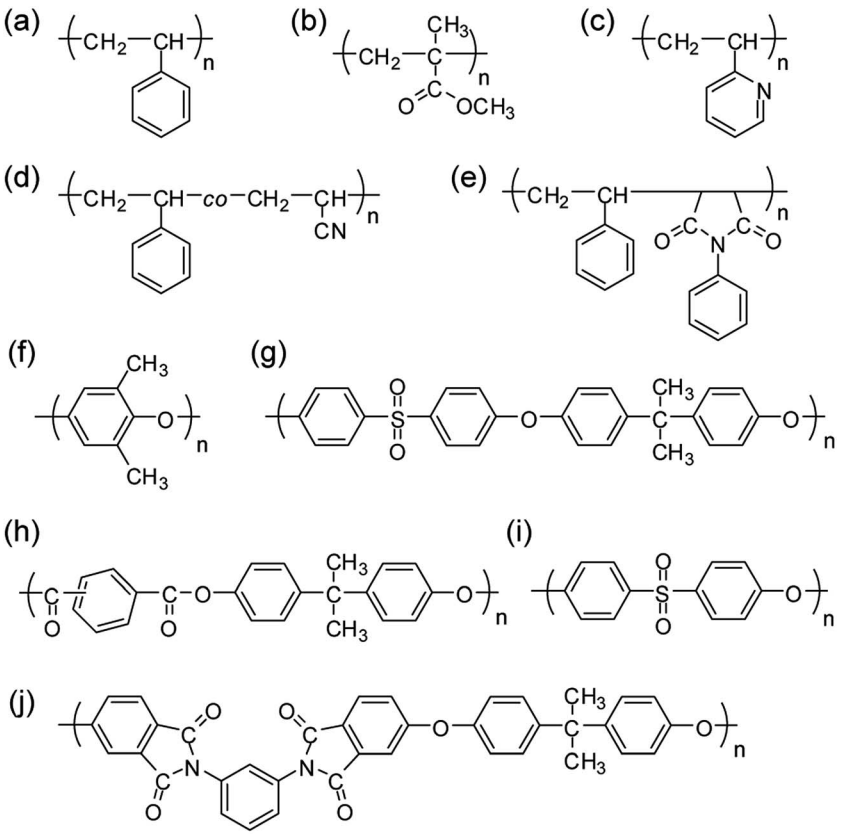

Fig. 1 Chemical structures of polymer matrices used in this study. (a) PS. (b) PMMA. (c) P2VP. (d) SAN. (e) St-PMI. (f) PPE. (g) PSF. (h) PAR. (i) PES. (j) PEI.

Table 1 Dielectric characteristics (1 kHz) for polymer/α-Fe_2O_3 composites with $\Phi = 0.2$ obtained at 40 °C

Polymer	ε'_r	ε''_r	$\varepsilon'_{r\ polymer}$ [a]	$\varepsilon'_{r\ Fe_2O_3}$ [b]
PS	4.12	0.123	2.58	27.8
PMMA	5.25	0.453	3.39	31.2
P2VP	6.34	0.447	4.22	33.3
SAN	5.05	0.286	3.03	40.5
PSF	5.71	0.339	3.13	66.2
St-PMI	5.59	0.182	2.88	83.4
PAR	6.52	0.402	3.27	109
PEI	6.23	0.250	3.09	109
PES	7.13	0.475	3.52	116
PPE	5.58	0.162	2.63	120

[a] ε'_r of the polymer matrix only. [b] Apparent ε'_r of α-Fe_2O_3 calculated using Lichteneker's logarithmic mixing rule.

popular, and some of them are engineering plastics that can be used over 150 °C (Fig. 1f–j). The ε'_r and dielectric loss factor ε''_r values of the polymer/α-Fe_2O_3 composites (1 kHz, 40 °C) were listed in Table 1. There is a weak tendency for the ε'_r of the composites prepared using the engineering plastics to be high. This is an interesting phenomenon that has never been reported. However, it is difficult to correctly evaluate the ε'_r enhancement effect by direct comparing of the ε'_r values of the composites because each ε'_r of the polymer matrix $\varepsilon'_{r\ polymer}$ is different to some extent as shown in Table 1. Therefore, we suggest that apparent ε'_r of α-Fe_2O_3, $\varepsilon'_{r\ Fe_2O_3}$ is calculated using Lichteneker's logarithmic mixing rule and then compared in order to separate a contribution of the $\varepsilon'_{r\ polymer}$ itself from the ε'_r of the composite. It is known that the ε'_r of a polymer/filler composite often obeys Lichteneker's logarithmic mixing rule as follows:[4,7,9,15–17,39]

$$\varepsilon'_r = \varepsilon'_{r\ polymer}(\varepsilon'_{r\ filler}/\varepsilon'_{r\ polymer})^{\Phi}, \quad (1)$$

where $\varepsilon'_{r\ filler}$ and Φ are the ε'_r and volume fraction of the filler. Notice that the $\varepsilon'_{r\ filler}$ is not the ε'_r of the filler itself but an apparent ε'_r of the filler particles in the polymer matrix. Generally, the $\varepsilon'_{r\ filler}$ is much smaller than the ε'_r of the corresponding bulk compound, mainly because the filler particles do not form a continuous phase in the polymer/filler composite system; the $\varepsilon'_{r\ filler}$ is significantly reduced by the interface between the filler particles. Furthermore, the $\varepsilon'_{r\ filler}$ is affected not only by the size and form of the filler particle but also by the dispersivity of the filler particles in the matrix.[16] For example, the apparent ε'_r of spherical $BaTiO_3$ nanoparticles with a diameter of less than 100 nm is reported to be around 100 according to literatures.[8,39]

The calculated $\varepsilon'_{r\ Fe_2O_3}$ is shown in Table 1. There is a strong dependency of the $\varepsilon'_{r\ Fe_2O_3}$ on the polymer matrix; the $\varepsilon'_{r\ Fe_2O_3}$ is about 30 for PS, PMMA and P2VP whereas over 100 for PAR, PEI, PES and PPE. In other word, the ε'_r for engineering plastics is more enhanced by the α-Fe_2O_3 particles than that for general-purpose plastics such as PS and PMMA. Fig. 2 shows the frequency f dependences of the ε'_r and ε''_r of four kinds of composites for PEI, PSF, PPE and PS with $\Phi = 0.2$ obtained at 40 °C. Every ε'_r is decreased as f is increased. This is because the dielectric relaxation of a polarization occurs in the f range, which results in a ε''_r peak as shown in Fig. 2b. This polarization would be attributed to the interfacial polarization of free electrons in the α-Fe_2O_3 particles, that is Maxwell–Wagner polarization.[33] Because the relaxation frequency becomes high as the σ of the α-Fe_2O_3 particles is high for Maxwell–Wagner polarization, it is suggested that the σ of the α-Fe_2O_3 particles in the PEI/α-Fe_2O_3 and PPE/α-Fe_2O_3 composites is higher than that in the PS/α-Fe_2O_3 composite, resulting in the higher $\varepsilon'_{r\ Fe_2O_3}$ for PEI and PPE over the reported value of ~30.[22–27] This is probably because the π electrons in the aromatic structures of the engineering plastics strongly interact with the electrons in the α-Fe_2O_3 particles. Also, it is suggested that the enhanced $\varepsilon'_{r\ Fe_2O_3}$ is caused by the dispersivity of the α-Fe_2O_3 particles in the polymer matrix and the interfacial state between the α-Fe_2O_3 particles and the polymer matrix. However, it is difficult to explain the strong frequency dependence of the dielectric properties as shown in Fig. 2 by these two contributions (the dispersivity and the interfacial state). Therefore, we conclude

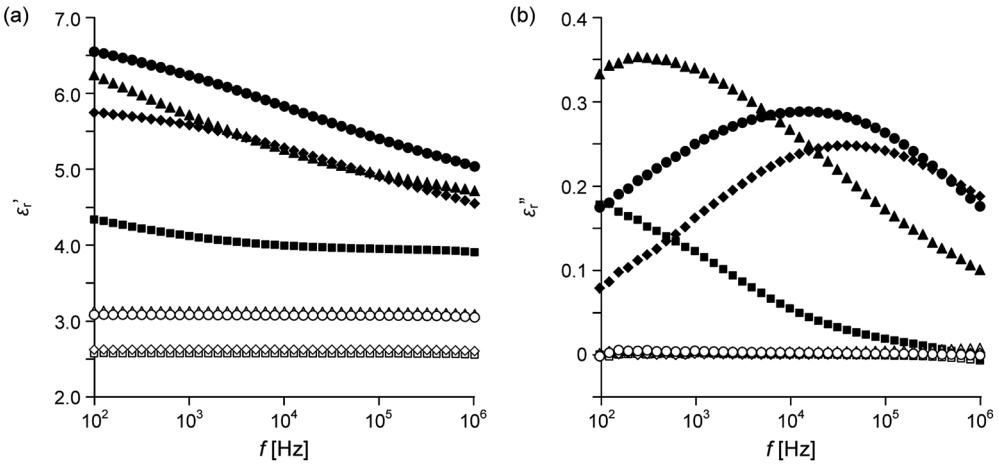

Fig. 2 Frequency f dependence of (a) ε'_r and (b) ε''_r of polymer/α-Fe_2O_3 composites with $\Phi = 0$ (open symbols) and $\Phi = 0.2$ (filled symbols) obtained at 40 °C. The polymer matrices are PEI (circles), PSF (triangles), PPE (diamonds) and PS (squares).

that the enhanced $\varepsilon'_{r\ Fe_2O_3}$ is mainly due to the interaction between the electrons in the α-Fe_2O_3 particles and the polymer matrix. From the viewpoint of the molecular structures of the polymer matrix, the α-Fe_2O_3 particles might be more effective for fully aromatic polyester and polyimide with long conjugations.

Dielectric properties of polymer/α-Fe_2O_3 composites at 160 °C

The PEI/α-Fe_2O_3 and PPE/α-Fe_2O_3 composites are not useful at 40 °C owing to the large ε''_r values over 0.1 (Table 1). Under an electric field E, the power loss of a dielectric material per unit volume, P is expressed as,[16]

$$P = E^2 \times 2\pi f \varepsilon_0 \varepsilon''_r, \quad (2)$$

where ε_0 is the permittivity of vacuum. Because P is proportional to ε''_r, the ε''_r of the material must be low for industrial applications such as capacitors.

The large ε''_r values of the polymer/α-Fe_2O_3 composites are drastically reduced at 160 °C. Dielectric characteristics (1 kHz) obtained at 160 °C were listed in Table 2 for six kinds of polymer/α-Fe_2O_3 composites with $\Phi = 0.2$. At 1 kHz, all the ε''_r values are less than 0.05. Furthermore, for PEI, PSF, PAR and PES, the $\varepsilon'_{r\ Fe_2O_3}$ is more than 150 at 160 °C. For the four kinds of composites, the f dependences of the ε'_r and ε''_r are shown in Fig. 3. Because the dielectric relaxations of Maxwell–Wagner polarization are not started at around 1 kHz as shown in Fig. 3b, the ε''_r values are small in the lower f ranges than 1 kHz. This result indicates the σ of the α-Fe_2O_3 particle is higher at 160 °C than 40 °C. Fig. 4 shows a variation in the f dependences of the ε'_r and ε''_r of the PEI/α-Fe_2O_3 composites with $\Phi = 0.2$ between 40 and 160 °C. The ε''_r peak is shifted to the higher f until the temperature reaches 120 °C.

Table 2 Dielectric characteristics (1 kHz) for polymer/α-Fe_2O_3 composites with $\Phi = 0.2$ obtained at 160 °C

Polymer	ε'_r	ε''_r	$\varepsilon'_{r\ polymer}$ [a]	$\varepsilon'_{r\ Fe_2O_3}$ [b]
St-PMI	5.95	0.0307	2.87	116
PPE	5.71	0.0110	2.61	139
PEI	6.73	0.0321	3.11	157
PSF	6.82	0.0525	3.12	165
PAR	7.29	0.0509	3.31	182
PES	8.32	0.0533	3.53	246

[a] ε'_r of the polymer matrix only. [b] Apparent ε'_r of α-Fe_2O_3 calculated using Lichteneker's logarithmic mixing rule.

For the four polymer matrices, we also prepared polymer/α-Fe_2O_3 composites with $\Phi = 0.4$. Fig. 5 shows the f dependences of the ε'_r and ε''_r of polymer/α-Fe_2O_3 composites with $\Phi = 0.4$ at 160 °C. The ε''_r of the PEI/α-Fe_2O_3 composite remains small whereas for PAR and PES, the ε''_r becomes very large over all the f range. In order to elucidate the large ε''_r, the volume resistivity ρ_{DC} of the composites was measured. At $\Phi = 0.4$, the ρ_{DC} for PAR and PES is much lower than that for PEI and PSF as shown in Fig. 6. ε''_r is the sum of a loss from σ, $\varepsilon''_{r(\sigma)}$ and losses from dielectric polarizations $\varepsilon''_{r(DP)}$:[40]

$$\varepsilon''_r = \varepsilon''_{r(\sigma)} + \varepsilon''_{r(DP)}. \quad (3)$$

Furthermore, $\varepsilon''_{r(\sigma)}$ is described using ρ_{DC} as follows:

$$\varepsilon''_{r(\sigma)} = 1/(2\pi f \varepsilon_0 \rho_{DC}). \quad (4)$$

It is suggested that because $\varepsilon''_{r(\sigma)}$ is inversely proportion to f and ρ_{DC}, the ε''_r is highly increased at the low f range for PAR and PES. The low ρ_{DC} for PAR and PES could be attributed to a leak current passing through the conductive networks of the α-Fe_2O_3 particles, that is, percolation of the α-Fe_2O_3 particles. According to the percolation theory with a random packing of spherical particles, the percolation threshold is calculated to be about 0.30.[41,42] Therefore, it was reasonable that the percolation of the α-Fe_2O_3 particles occurred in the polymer/α-Fe_2O_3 composites with $\Phi = 0.4$. To the contrary, it was unusual that the PEI/α-Fe_2O_3 composite had a high ρ_{DC} even at $\Phi = 0.4$. We suspected that the dispersivity of the α-Fe_2O_3 particles in the polymer matrix was different between

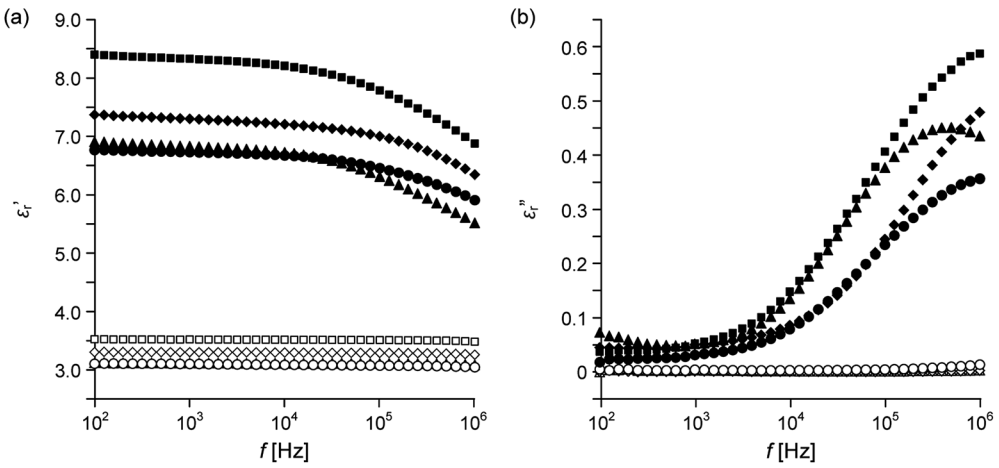

Fig. 3 Frequency f dependence of (a) ε'_r and (b) ε''_r of polymer/α-Fe_2O_3 composites with $\Phi = 0$ (open symbols) and $\Phi = 0.2$ (filled symbols) obtained at 160 °C. The polymer matrices are PEI (circles), PSF (triangles), PAR (diamonds) and PES (squares).

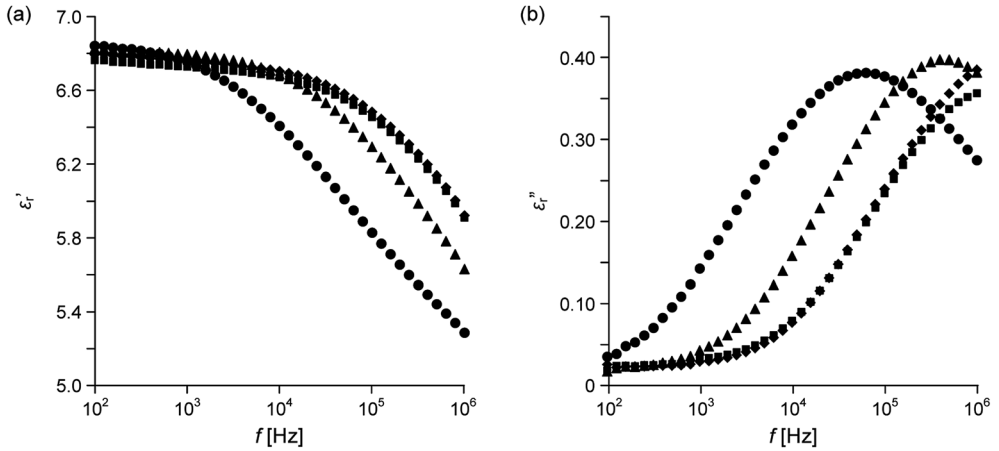

Fig. 4 Frequency f dependence of (a) ε'_r and (b) ε''_r of a PEI/α-Fe_2O_3 composite with $\Phi = 0.2$ obtained at 40 °C (circles), 80 °C (triangles), 120 °C (diamonds) and 160 °C (squares).

the PEI/α-Fe_2O_3 and PAR/α-Fe_2O_3 composites, and observed it using SEM. Fig. 7 shows SEM images of the PEI/α-Fe_2O_3 and PAR/α-Fe_2O_3 composites with $\Phi = 0.20$ and $\Phi = 0.4$. There is no great difference in the dispersivity of the α-Fe_2O_3 particles, which means that the significant difference in ρ_{DC} is not due to the dispersivity of the α-Fe_2O_3 particles. In the PEI/α-Fe_2O_3 composite, the α-Fe_2O_3 particles would be covered with a PEI layer at a nanometer scale, resulting in the high ρ_{DC} for PEI owing to inhibition of the tunneling conduction of the free electron[39,43] between the α-Fe_2O_3 particles.

Comparing of dielectric performance for PEI/α-Fe_2O_3 and PEI/$BaTiO_3$ composites

As mentioned above, the PEI/α-Fe_2O_3 composite exhibits the high ε'_r and very low ε''_r at the elevated temperature above 120 °C, which might be promising as a low-cost dielectric material for high-temperature applications; PEI has a maximum operating temperature of 200 °C.[35] Therefore, the novel PEI/α-Fe_2O_3 composite was compared with a conventional PEI/$BaTiO_3$

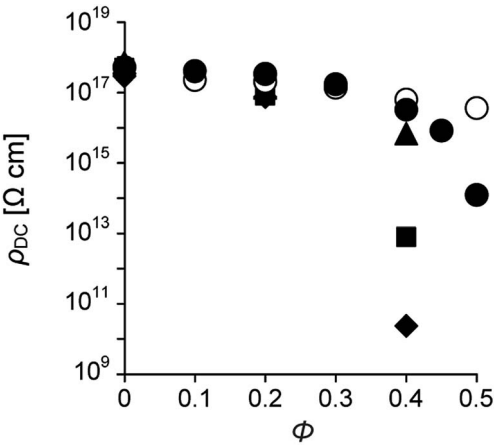

Fig. 6 Volume resistivity ρ_{DC} of polymer/α-Fe_2O_3 (filled symbols) and PEI/$BaTiO_3$ (open symbols) composites as a function of Φ. The polymer matrices are PEI (circles), PSF (triangles), PAR (diamonds) and PES (squares).

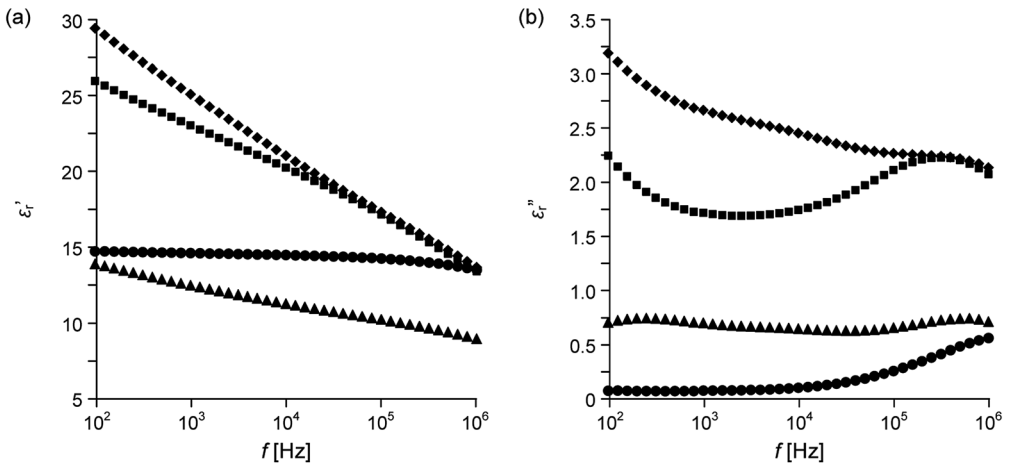

Fig. 5 Frequency f dependence of (a) ε'_r and (b) ε''_r of polymer/α-Fe_2O_3 composites with $\Phi = 0.4$ obtained at 160 °C. The polymer matrices are PEI (circles), PSF (triangles), PAR (diamonds) and PES (squares).

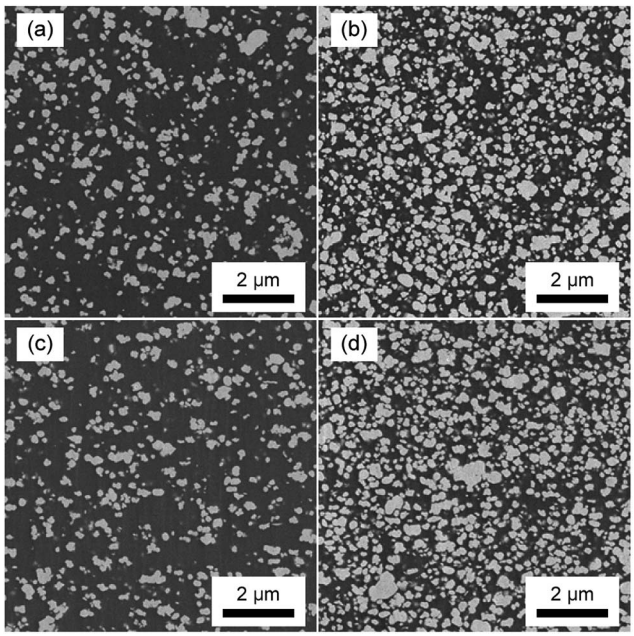

Fig. 7 SEM images of (a and b) PEI/α-Fe_2O_3 and (c and d) PAR/α-Fe_2O_3 composites with (a and c) $\Phi = 0.2$ and (b and d) $\Phi = 0.4$.

composite in dielectric performance. As shown in Fig. 6, the ρ_{DC} values of both the composites are comparable at room temperature when Φ is less than 0.4, whereas the ρ_{DC} of PEI/α-Fe_2O_3 is much lower than that of PEI/$BaTiO_3$ at the higher Φ. This is because the interparticle distance becomes small enough for tunneling conduction to occur owing to high loading of particles. Fig. 8 shows the f dependences of the ε'_r and ε''_r of the two types of composites obtained at 40 °C and 160 °C. At 40 °C, although the ε'_r of PEI/α-Fe_2O_3 is higher than that of PEI/$BaTiO_3$ in the lower f range, the ε''_r of PEI/α-Fe_2O_3 is much larger than that of PEI/$BaTiO_3$. At 160 °C, however, ε'_r has comparable ε''_r values to PEI/$BaTiO_3$ except with $\Phi = 0.5$, and higher ε'_r than PEI/$BaTiO_3$. The dielectric characteristics at 1 kHz obtained at 160 °C are plotted as a function of Φ in Fig. 9. These results show that the PEI/α-Fe_2O_3 composite was comparable to the PEI/$BaTiO_3$ composite in dielectric performance at 160 °C. The fitting curves for the ε'_r of the two types of composites are drawn in Fig. 9a in solid lines using Lichteneker's logarithmic mixing rule. These theoretical curves well fit to the experimental results and give $\varepsilon'_{r\ BaTiO_3}$ of 86 and $\varepsilon'_{r\ Fe_2O_3}$ of 170, respectively. This value of 86 for $BaTiO_3$ is

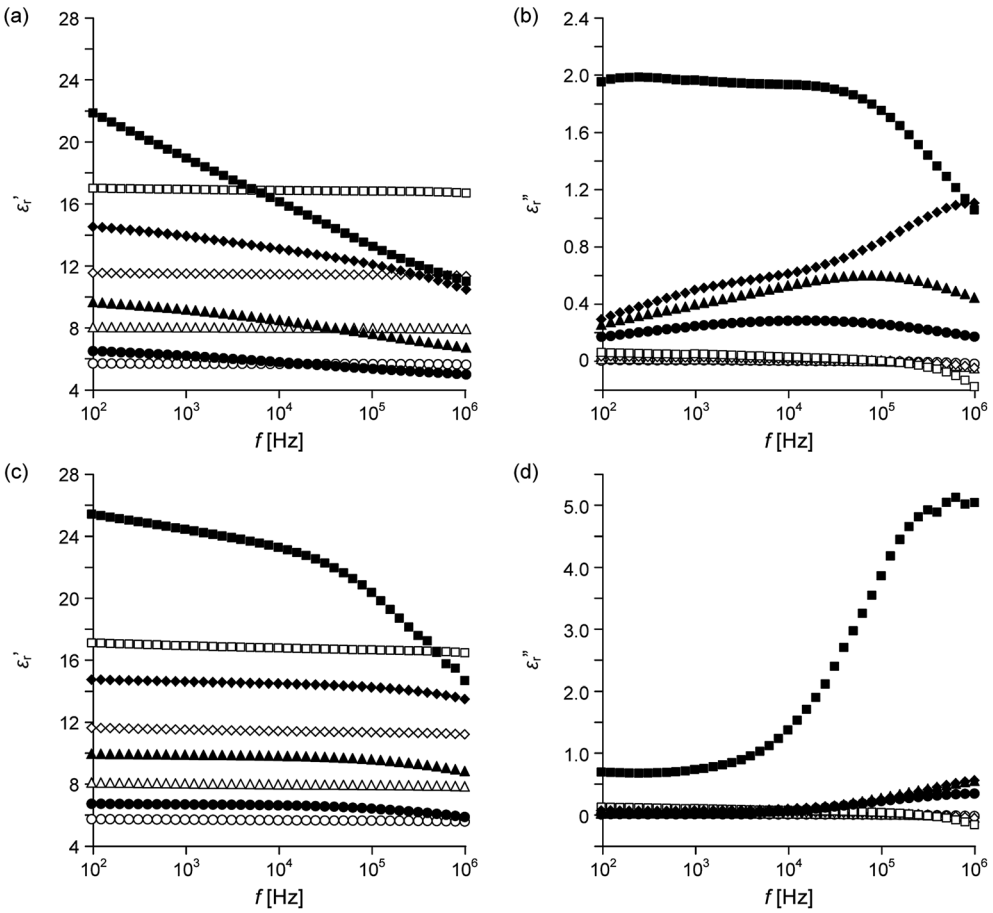

Fig. 8 Frequency f dependence of (a and c) ε'_r and (b and d) ε''_r of two types of composites with $\Phi = 0.2$ (circles), $\Phi = 0.3$ (triangles), $\Phi = 0.4$ (diamonds) and $\Phi = 0.5$ (squares) obtained at (a and b) 40 °C and (c and d) 160 °C. Open symbols, PEI/$BaTiO_3$; filled symbols, PEI/α-Fe_2O_3.

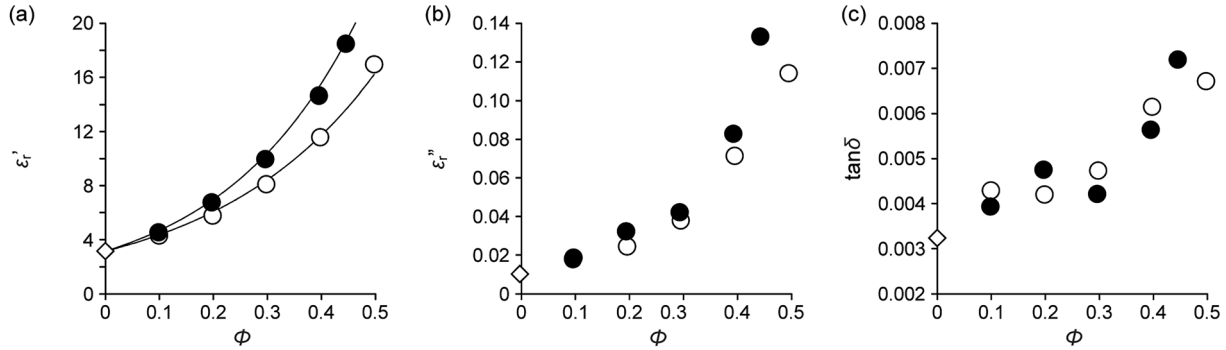

Fig. 9 (a) ε'_r, (b) ε''_r and (c) dissipation factor (tan δ) (1 kHz) of PEI (diamonds) and two types of composites (circles) obtained at 160 °C as a function of Φ. Open symbols, PEI/$BaTiO_3$; filled symbols, PEI/α-Fe_2O_3. (a) Solid lines show the fitting curves using Lichtenecker's logarithmic mixing rule.

consistent with some reported results; $\varepsilon'_{r\ BaTiO_3}$ is around 100.[8,39]

Conclusion

The dielectric properties of polymer/α-Fe_2O_3 composites strongly depended not only on the temperatures but also on the kind of polymer matrices. For engineering plastics such as PEI, PSF, PAR and PES, the ε'_r was highly enhanced at around 1 kHz by incorporation of α-Fe_2O_3 particles owing to Maxwell–Wagner polarization of free electrons in the α-Fe_2O_3 particles. This is probably because the π electrons in the aromatic structures of the engineering plastics strongly interact with the electrons in the α-Fe_2O_3 particles. Furthermore, the ε''_r for the engineering plastics became small at the elevated temperatures because the σ of the α-Fe_2O_3 particle was enhanced and therefore the relaxation frequency of Maxwell–Wagner polarization was shifted to higher f. PEI/α-Fe_2O_3 composites exhibited highly improved dielectric properties at around 1 kHz, the high ε'_r and very low ε''_r at the elevated temperature above 120 °C. It was demonstrated that the PEI/α-Fe_2O_3 composite was comparable to the PEI/$BaTiO_3$ composite in dielectric performance at 160 °C. Because the cost of α-Fe_2O_3 is much lower than that of $BaTiO_3$, the PEI/α-Fe_2O_3 composites might be promising as a low-cost dielectric material for high-temperature applications.

Acknowledgements

SEM observation was carried out by Mr Yasuhiro Takatani at Toyota Central R&D Labs Inc. The authors appreciate his help.

References

1 W. J. Sarjeant, J. Zirnheld, F. W. MacDougall, J. S. Bowers, N. Clark, I. W. Clelland, R. A. Price, M. Hudis, I. Kohlberg, G. McDuff, I. McNab, S. G. Parler Jr and J. Prymak, in *Handbook of low and high dielectric constant materials and their applications*, ed. H. S. Nalwa, Academic Press, London, 1999, vol. 2, ch. 9, pp. 423–491.
2 Q. Wang and L. Zhu, *J. Polym. Sci., Part B: Polym. Phys.*, 2011, **49**, 1421–1429.
3 Z. M. Dang, J. K. Yuan, J. W. Zha, T. Zhou, S. T. Li and G. H. Hu, *Prog. Mater. Sci.*, 2012, **57**, 660–723.
4 S. D. Cho, S. Y. Lee, J. G. Hyun and K. W. Paik, *J. Mater. Sci.: Mater. Electron.*, 2005, **16**, 77–84.
5 P. Kim, S. C. Jones, P. J. Hotchkiss, J. N. Haddock, B. Kippelen, S. R. Marder and J. W. Perry, *Adv. Mater.*, 2007, **19**, 1001–1005.
6 J. Lu and C. P. Wong, *IEEE Trans. Dielectr. Electr. Insul.*, 2008, **15**, 1322–1328.
7 K. W. Jang and K. W. Paik, *J. Appl. Polym. Sci.*, 2008, **110**, 798–807.
8 P. Kim, N. M. Doss, J. P. Tillotson, P. J. Hotchkiss, M. J. Pan, S. R. Marder, J. Li, J. P. Calame and J. W. Perry, *ACS Nano*, 2009, **3**, 2581–2592.
9 Y. Kobayashi, A. Kurosawa, D. Nagao and M. Konno, *Polym. Eng. Sci.*, 2009, **49**, 1069–1075.
10 A. Choudhury, *Mater. Chem. Phys.*, 2010, **121**, 280–285.
11 L. Xie, X. Huang, C. Wu and P. Jiang, *J. Mater. Chem.*, 2011, **21**, 5897–5906.
12 S. Siddabattuni, T. P. Shuman and F. Dogan, *Mater. Sci. Eng., B*, 2011, **176**, 1422–1429.
13 M.-F. Lin, V. K. Thakur, E. J. Tan and P. S. Lee, *RSC Adv.*, 2011, **1**, 576–578.
14 Y. Song, Y. Shen, H. Liu, Y. Lin, M. Li and C. W. Nan, *J. Mater. Chem.*, 2012, **22**, 16491–16498.
15 X. Wu, Z. Chen and Z. Cui, *Compos. Sci. Technol.*, 2013, **81**, 48–53.
16 K. Hayashida and Y. Matsuoka, *Carbon*, 2012, **60**, 506–513.
17 K. Hayashida, Y. Matsuoka and Y. Takatani, *RSC Adv.*, 2014, **4**, 33530–33536.
18 C. Fettkenhauer, J. Glenneberg, W. Münchgesang, H. S. Leipner, G. Wagner, M. Diestelhorst, C. Pientschke, H. Beige and S. G. Ebbinghaus, *RSC Adv.*, 2014, **4**, 40321–40329.
19 W. Lei, R. Wang, D. Yang, G. Hou, X. Zhou, H. Qiao, W. Wang, M. Tian and L. Zhang, *RSC Adv.*, 2015, **5**, 47429–47438.

20 W. Yang, S. Yu, S. Luo, R. Sun, W.-H. Liao and C.-P. Wong, *J. Alloys Compd.*, 2015, **620**, 315–323.
21 Y. Feng, W. L. Li, Y. F. Hou, Y. Yu, W. P. Cao, T. D. Zhang and W. D. Fei, *J. Mater. Chem. C*, 2015, **3**, 1250–1260.
22 R. B. Hilborn Jr, *J. Appl. Phys.*, 1965, **36**, 1553–1557.
23 K. Iwauchi, S. Yamamoto, Y. Bando and N. Koizumi, *Bull. Inst. Chem. Res., Kyoto Univ.*, 1970, **48**, 159–169.
24 D. A. Sverjensky and N. Sahai, *Geochim. Cosmochim. Acta*, 1996, **60**, 3773–3797.
25 M. L. Jimenez, F. J. Arroyo, F. Carrique and U. Kaatze, *J. Phys. Chem. B*, 2003, **107**, 12192–12200.
26 J. A. Glasscock, P. R. F. Barnes, I. C. Plumb, A. Bendavid and P. J. Martin, *Thin Solid Films*, 2008, **516**, 1716–1724.
27 R. A. Lunt, A. J. Jackson and A. Walsh, *Chem. Phys. Lett.*, 2013, **586**, 67–69.
28 D. Dudić, M. Marinović-Cincović, J. M. Nedeljković and V. Djoković, *Polymer*, 2008, **49**, 4000–4008.
29 A. M. E. Sayed and W. M. Morsi, *J. Mater. Sci.*, 2014, **49**, 5378–5387.
30 D. Chen, H. Quan, Z. Huang, S. Luo, X. Luo, F. Deng, H. Jiang and G. Zeng, *Compos. Sci. Technol.*, 2014, **102**, 126–131.
31 C. Kittel, in *Introduction to Solid State Physics*, ed. C. Kittel, John Wiley & Sons, New York, 7th edn, 1996, ch. 8, pp. 197–232.
32 S. Mohanty and J. Ghose, *J. Phys. Chem. Solids*, 1992, **53**, 81–91.
33 A. Schönhals and F. Kremer, in *Broadband Dielectric Spectroscopy*, ed. F. Kremer and A. Schönhals, Springer-Verlag, Berlin, 2003, ch. 3, pp. 59–98.
34 D. Tan, L. Zhang, Q. Chen and P. Irwin, *J. Electron. Mater.*, 2014, **43**, 4569–4575.
35 Q. Li, L. Chen, M. R. Gadinski, S. Zhang, G. Zhang, H. Li, A. Haque, L. Q. Chen, T. Jackson and Q. Wang, *Nature*, 2015, **523**, 576–580.
36 M. N. Teerenstra, P. A. M. Steeman, W. Iwens, A. Vandervelden, D. R. Suwier, B. V. Mele and C. E. Koning, *e-Polym.*, 2003, **3**, 596–607.
37 H.-B. Tsai and Y.-D. Lee, *J. Polym. Sci., Part A: Polym. Chem.*, 1987, **25**, 1505–1515.
38 N. Erdman, R. Campbeli and S. Asahina, *Microsc. Today*, 2006, **14**, 22–25.
39 K. Hayashida, *RSC Adv.*, 2013, **3**, 221–227.
40 K. Hayashida and Y. Matsuoka, *Carbon*, 2015, **85**, 363–371.
41 G. E. Pike and C. H. Seager, *Phys. Rev. B: Solid State*, 1974, **10**, 1421–1434.
42 C. D. Lorenz and R. M. Ziff, *J. Chem. Phys.*, 2001, **114**, 3659–3661.
43 K. Hayashida and H. Tanaka, *Adv. Funct. Mater.*, 2012, **22**, 2338–2344.